

Additional enhancement in surface-enhanced Raman scattering due to excitation geometry

Lorenzo Rosa^a, Sasani Jayawardhana^b, Saulius Juodkazis^{a,c}, Paul R. Stoddart^{*b}

^aCentre for Micro-Photonics, Swinburne University of Technology, John Street, Hawthorn, Victoria 3122, Australia;

^bFaculty of Engineering & Industrial Science, Swinburne University of Technology, John Street, Hawthorn, Victoria 3122, Australia

^cMelbourne Centre for Nanofabrication, 151 Wellington Road, Clayton, VIC 3168, Australia

ABSTRACT

It is well known that surface-enhanced Raman scattering (SERS) substrates based on metal island films exhibit higher levels of enhancement when excited through a transparent base material than when excited directly through air. However, to our knowledge, the origin of this enhancement has never been satisfactorily explained. An initial suggestion that the additional enhancement was due to a “nearest layer effect” cannot account for the observation of additional enhancement for monolayer adsorbates. In this paper, finite difference time domain (FDTD) modelling is presented to show that the electric field intensity in between metal particles at the interface is higher for “far-side” excitation. This is reasonably consistent with the observed enhancement for silver islands on SiO₂. The modelling results are in agreement with a simple physical model based on Fresnel reflection at the interface. This suggests that the additional enhancement is due to a near-field enhancement of the electric field due to the phase shift at the dielectric interface, when the light passes from the higher to the lower region of refractive index.

Keywords: Surface-enhanced Raman scattering, Fresnel reflection, finite difference time domain

INTRODUCTION

Surface-enhanced Raman scattering provides a sensitive method for detecting trace levels of a wide range of chemical compounds.^{1,2} The process is related to normal Raman scattering, where a small fraction of incident laser light is inelastically scattered by molecular vibrational modes of the target material. Typical cross sections for Raman scattering are 10⁻³⁰ cm², which is substantially lower than fluorescence yields of 10⁻¹⁴ cm².³ In surface enhanced Raman scattering, it has been shown that the scattering intensity can be increased by a factor of 10⁶ or more if the target molecules are adsorbed onto the nanostructured surface of an appropriate metal. The most commonly used metals include silver, gold and copper. The enhancement arises primarily from the enhanced electromagnetic field produced by resonant excitation of the surface electrons in the metal nanostructures,⁴ although a “chemical” enhancement mechanism has also been proposed due to charge transfer interactions with the metal.⁵

A number of different methods have been proposed for the fabrication of nanostructured metal surfaces suitable for SERS.^{1-3,6} In many cases, metal particles are deposited on a dielectric substrate, which is typically glass. In general, the resulting SERS substrate is then excited from the “air” side in a backscatter geometry. Efforts to identify alternative measurement geometries have led to several reports that a larger SERS signal is obtained by excitation through the dielectric medium than by excitation through air.⁷⁻¹⁰ Jennings et al.⁹ reported the use of glass slides with vacuum deposited silver/indium island films and a 90° scattering geometry. They did not quantify the extra enhancement, but suggested a ‘first layer effect’, where the analyte layer that is closest to the enhancement field generates a higher signal. However, this argument appears to have fallen out of favour in later work.¹⁰ In the absence of a convincing mechanism, this additional enhancement appears to have been relatively neglected since then.

*pstoddart@swin.edu.au

EXPERIMENTAL RESULTS

Glass cover slips with a 100- μm thickness were used without any surface pretreatment to investigate the excitation of a SERS substrate in the direct and reverse directions. The cover slips were mounted on a glass slide and placed in the Emitech K975X thermal evaporator unit. A 2-nm chromium adhesion layer was sputtered onto the exposed surface of the cover slip prior to laying down a silver island film by oblique angle deposition (OAD). A nominal deposition thickness of 100 nm of silver was coated on the sample at an angle of 86° and a deposition rate of $0.05 \text{ nm}\cdot\text{s}^{-1}$. This procedure produces a thin metal island film on the surface of the cover slip.^{11,12}

The cover slips with the OAD nanostructure were then functionalized with thiophenol, which is commonly used as a SERS reference because it forms a stable self assembled monolayer on the metal surface.¹² The thiophenol SERS spectra were acquired with an InVia Streamline microscope (Renishaw, UK). Measurements were taken using several different microscope objectives, which provided a range of collection apertures. The near-side and far-side measurement geometries are shown in Figure 1. The average intensity of the four main thiophenol peaks (1000 , 1021 , 1072 and 1573 cm^{-1}) is plotted against the solid angle of signal collection in Figure 2. The data was adjusted for the laser power at the sample for each objective. As observed from Figure 2, the intensity of the SERS signals collected from the far-side excitation is higher than that collected from the near-side interrogation, across all objectives. At low NA objectives this ratio is approximately 3 and it decreases for higher NA objectives.

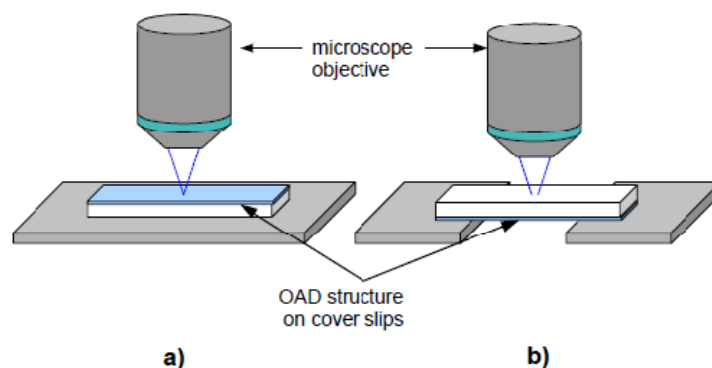


Figure 1. Cover slips coated with silver using OAD and measured for SERS in a) near-side interrogation and b) far-side interrogation.

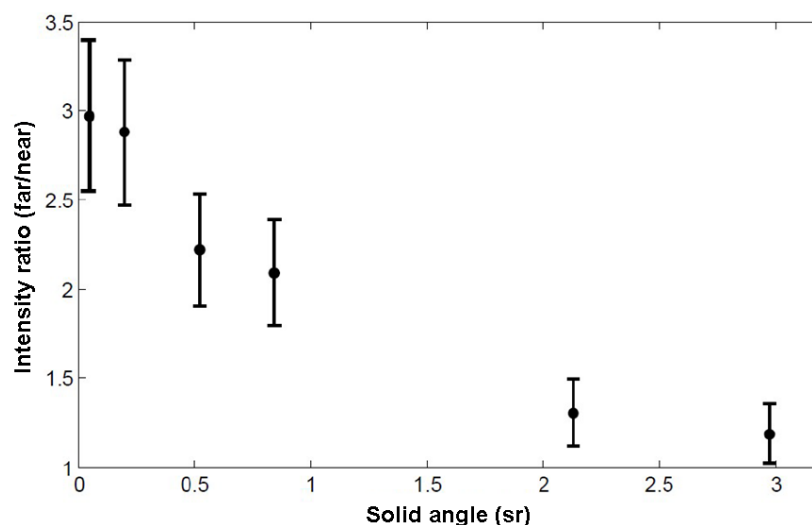


Figure 2. The ratio between far-side and near-side measurements taken from the same SERS substrate for a range of microscope objectives. The intensity values were based on the average intensity of the four main peaks in the thiophenol spectrum.

FDTD MODELLING

In order to understand the additional enhancement observed in the reverse geometry, 3D-FDTD simulations were carried out with the FDTD Solutions software (Lumerical Solutions, Inc.) to evaluate the field enhancement produced in the nanogap between hemispherical particles, as shown in Figure 3. A SiO₂ slab of 1 μm thickness is positioned inside the domain, and hemispherical silver nanoparticles of 30 nm diameter and 15 nm height have been paired, leaving a nanogap width of 6 nm. These dimensions are based on SEM analysis of the silver island films used in the SERS experiment. The nanoparticles are placed in two pairs, one on the slab side closest to the light source (near side) and one on the opposite (far) side. The pairs are spaced by 1 μm along the x-axis, which is enough to gather data on both pairs in the same simulation without mutual interference. The domain size is 1 × 1 × 2 μm³, illuminated by an x-polarized plane wave light source with bandwidth from 350 to 650 nm wavelength. Periodic boundary conditions are placed on the x- and y-boundaries to avoid plane wave diffraction at the domain edges. The silver and silica materials are modeled in the Lumerical database by time-domain polynomial fitting of the tabulated experimental (*n*, *k*) spectra according to Palik.¹³

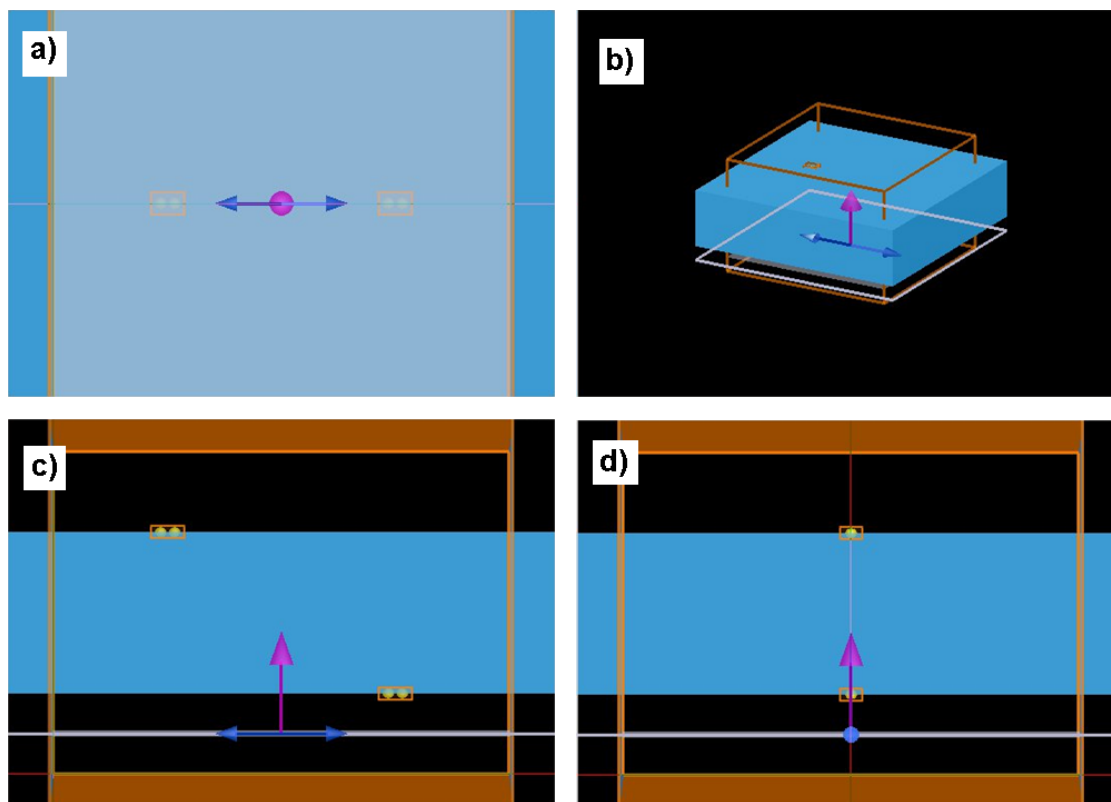


Figure 3. FDTD modeling domain (brown cube) comprising a silica slab of 1 μm thickness (in blue) and two pairs of hemispherical silver nanoparticles, positioned at 1 μm spacing on the near side (x-positive) and far side (x-negative) with respect to the x-polarized plane wave source (white square). Projections are shown for (a) xy-plane, (b) 3D perspective, (c) xz-plane, and (d) yz-plane.

A single broadband field enhancement peak is found at 440 nm wavelength, where hot-spots are found in the middle of the nanogap at the interface between silver and silica. In Figure 4 the electric field intensity distribution (E^2) is shown at the peak wavelength, on matching yz-parallel planes bisecting the nanogaps on the respective sides. On the near side, the field enhancement on the glass surface (normalized to source intensity) peaks at 220, while on the far side it peaks at 400. The SERS signal is generally considered proportional to the fourth power of the electric field.^{1,14} Therefore the ratio of the SERS signals arising from this hot spot is given by $(E_{\text{far}}/E_{\text{near}})^4 \sim 3.31$. This is reasonably close to the experimental value of 3 found for a finite collection aperture in the previous section. The use of a finite collection aperture is not exactly comparable to the plane wave case, but is unavoidable in this experimental set-up as the signal tends to zero as the collection aperture tends to zero. Note that there is some evidence that the SERS signal tends to be dominated by scattering from hot spots such as the nanogap considered in this model.¹⁵

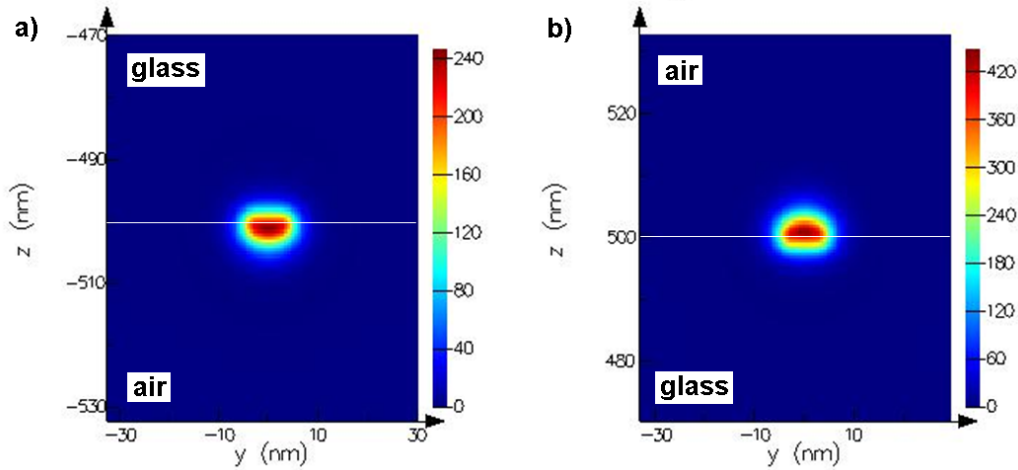


Figure 4. Electric field intensity distribution (values normalized to plane wave source intensity) at 440 nm wavelength on a yz-parallel plane positioned in mid-nanogap between the two particles on (a) near side and (b) far side.

FRESNEL MECHANISM

According to the Fresnel formulas for right angle incidence ($\theta_i = 0$), the coefficients of the in-plane (\parallel) polarized amplitudes of transmitted and reflected electric fields are, respectively:¹⁶

$$t_{\parallel} = \frac{2n_i}{n_i + n_t}, \quad r_{\parallel} \equiv 1 - t_{\parallel} = \frac{n_t - n_i}{n_i + n_t}$$

where $n_{i,t}$ are the refractive indices of the material on the incidence and transmission sides, respectively. The field component perpendicular to the plane of incidence is $t_{\perp} = t_{\parallel}$ and $r_{\perp} = -r_{\parallel}$, while the corresponding intensities are r^2 and t^2 . An E-field enhancement occurs when light passes from the medium with a larger refractive index to the medium with lower refractive index. In the case of a glass-air boundary ($n_i = 1.5$, $n_t = 1$) the transmitted field is enhanced by a factor of $t = (3/2.5) = 1.2$, while for an air-glass boundary loss occurs in transmission $t = (2/2.5) = 0.8$ when the incident field is $|\mathbf{E}| = 1$. Hence, a 20% gain at the exit interface can be obtained for the light passing through the glass plate. The physical reason for this enhancement is the phase shift at the boundary.

The energy (intensity) conservation condition $T + R = 1$ is fulfilled in the far-field as $(n_t/n_i)t^2 + r^2 = 1$. This is illustrated in Figure 5(a) and (b) and is irrespective of the direction of light propagation: from high-to-low index material or vice versa. Interestingly, if only the E-field is considered at the interface, a strong enhancement occurs when light traverses from a high-refractive medium to low, as shown in Figure 5(d). The far-field conservation of energy (intensity) does not forbid a significant local E-field enhancement in this case. In the SERS experiments this situation corresponds to the far-side excitation (through the sample). From this argument it would appear that an additional SERS enhancement of $E^4 \sim t^4 = 2.01$ is achievable on the far-side surface of silica substrates ($n = 1.47$) patterned with plasmonic nanostructures. For the realistic experimental situation when light intensity on the front plane is $I = 1$ in air, the intensity incident on the back plane is $(1-R)I = 0.964$ inside silica. Hence, the far-side SERS enhancement is $E^4 \sim ((1-R)^{1/2}t)^4 = 1.86$ i.e. a bit less than 2.0 as would be expected in comparison to a light source positioned inside the glass. The ratio between far-side and near-side enhancements is found to be 4.3, which compares favourably with both FDTD results and the observed enhancement ratio for silver island films on planar silica substrates.

The analysis presented above for plane wave propagation through a boundary from high to low refractive index shows a generic property of the light field enhancement (when the field amplitude is considered rather than intensity).

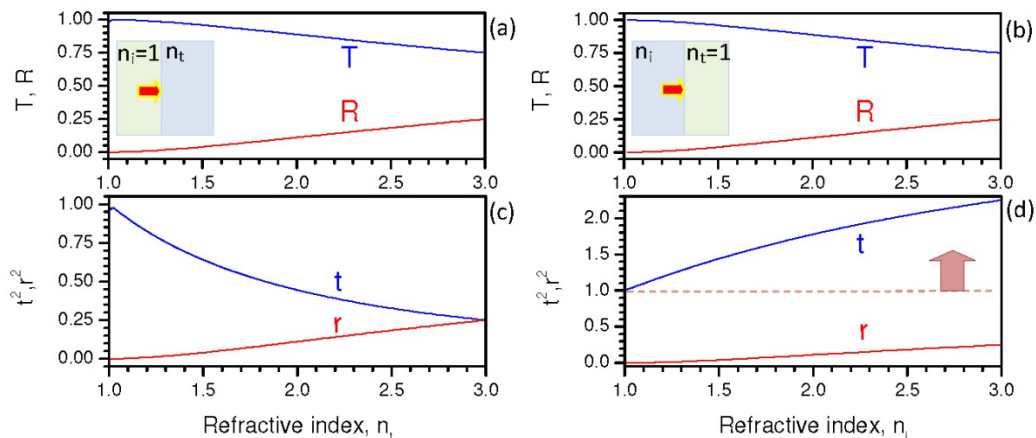


Figure 5. Fresnel enhancement: field intensity and amplitude transmission and reflection coefficients $T;R$ (a,b) and $t^2; r^2$, (c,d) respectively, at the interfaces. Inset schematically show the near-side (a,c) and far-side (b,d) sensing in the case of SERS. The arrow in (d) shows the field enhancement (note the different scales on the ordinate axis).

CONCLUSION

Fresnel enhancement of the E-field can be used to increase the signal intensity in SERS experiments. The observed SERS enhancement in the case of far-side excitation is quantitatively explained, within the limitations of the current experimental results. The explanation is consistent with literature data reported over the last 20 years. Further work is required to explore this effect in other substrate materials and to understand how surface roughness and the metal islands themselves affect the Fresnel factor. The angle dependence of the effect must also be investigated in order to account for practical situations where a range of excitation and scattering angles are involved. Nevertheless, this additional Fresnel enhancement may be significant in optical fibre SERS⁴ and other sensor devices where the collection aperture may be limited in comparison to Raman microscope systems. There are also push-pull forces exerted onto the interfaces due to the very same Fresnel scaling laws, since $Force = Power/c$, where c is velocity of light inside the medium. As light passes throughout the boundary, mechanical force is applied.^{17,18} This might affect molecular alignment and stretching of analyte species and be utilized for further control over the SERS signal.

ACKNOWLEDGMENTS

This work was supported by the Australian Research Council under Discovery Project grant DP1092955.

REFERENCES

- [1] Stiles, P. L., Dieringer, J. A., Shah, N. C. and Van Duyne, R. R., "Surface-enhanced Raman spectroscopy," *Annu. Rev. Anal. Chem.* 1, 601–626 (2008).
- [2] Kneipp, J., Wittig, B., Bohr, H. and Kneipp, K., "Surface-enhanced Raman scattering: a new optical probe in molecular biophysics and biomedicine," *Theor. Chem. Acc.* 125, 319-327 (2009).
- [3] Baker, G. A. and Moore, D. S., "Progress in plasmonic engineering of surface-enhanced Raman-scattering substrates toward ultra-trace analysis," *Anal. Bioanal. Chem.* 382 (8), 1751-1770 (2005).
- [4] Moskovits, M., "Surface-enhanced Raman spectroscopy: a brief retrospective," *J. Raman. Spectrosc.* 36(6-7), 485-496 (2005).
- [5] Otto, A., "The 'chemical' (electronic) contribution to surface-enhanced Raman scattering," *J. Raman. Spectrosc.* 36(6-7), 497-509 (2005).

- [6] Stoddart, P. R. and White, D. J., "Optical fibre SERS sensors," *Anal. Bioanal. Chem.* 394(7), 1761-1774 (2009).
- [7] Bello, J. M., Stokes, D. L. and Vo-Dinh, T., "Titanium-dioxide based substrate for optical monitors in surface-enhanced Raman-scattering analysis," *Anal. Chem.* 61 (15), 1779-1783 (1989).
- [8] Vo-Dinh, T., Miller, G. H., Bello, J., Johnson, R., Moody, R. L., Alak, A. and Fletcher, W. R., "Surface-active substrates for Raman and luminescence analysis," *Talanta* 36, 227-234 (1989).
- [9] Jennings, C., Aroca, R., Hor, A. M. and Loutfy, R. O., "Surface-enhanced Raman scattering from copper and zinc phthalocyanine complexes by silver and indium island films," *Anal. Chem.* 56, 2033-2035 (1984).
- [10] Aroca, R., Jennings, C., Kovacs, G. K., Loutfy, R. O. and Vincett, P. S., "Surface-enhanced Raman scattering of Langmuir-Blodgett monolayers of phthalocyanine by indium and silver island films," *J. Phys. Chem.* 89, 4051-4054 (1985).
- [11] Driskell, J. D., Shanmukh, S., Liu, Y., Chaney, S. B., Tang, X. J., Zhao, Y.P. and Dluhy, R. A., "The use of aligned silver nanorod arrays prepared by oblique angle deposition as surface enhanced Raman scattering substrates," *J. Phys. Chem. C* 112, 895-901 (2008).
- [12] Jayawardhana, S., Kostovski, G., Mazzolini, A. P., Stoddart, P. R., "Optical fiber sensor based on oblique angle deposition," *Appl. Opt.* 50, 155-162 (2011).
- [13] Palik, E. D. (editor), [Handbook of Optical Constants of Solids], Academic Press (1991)
- [14] Kerker, M., Wang, D. S. and Chew, H., "Surface enhanced Raman scattering (SERS) by molecules adsorbed at spherical particles," *Appl. Optics* 19, 4159-4174 (1980).
- [15] McMahon, J. M., Henry, A. I., Wustholz, K. L., Natan, M. J., Freeman, R. G., Van Duyne, R. P. and Schatz, G. C., "Gold nanoparticle dimer plasmonics: finite element method calculations of the electromagnetic enhancement to surface-enhanced Raman spectroscopy," *Anal. Bioanal. Chem.* 394(7), 1819-1825 (2009).
- [16] Hecht, E., [Optics], 4th ed., (2002).
- [17] Juodkasis, S., Murazawa, N., Wakatsuki, H. and Misawa, H., "Laser irradiation induced disintegration of a bubble in a glass melt," *Appl. Phys. A* 87(1), 41-45 (2007).
- [18] Murazawa, N., Juodkasis, S., Misawa, H. and Wakatsuki, H., "Laser trapping of deformable objects," *Opt. Express* 15(20), 13310-13317 (2007).